Proceedings of the 9th International Conference on Inventive Computation Technologies (ICICT-2026)
DVD Part Number: CFP26F70-DVD; ISBN: 979-8-3315-6916-7

Cloud-Enabled Preprocessing and Feature Extraction Framework for Hydrocephalus Detection from MRI Scans

R.B.Maria Sofia
Research Scholar, Department of Computer Science,
School of Computing Sciences, Vels Institute of Science,Technology and Advanced Studies
& Assistant Professor, Department of Computer Applications,
Christ college of Arts&Science, Kilachery, Tamil Nadu,
mariasofia.britto@gmail.com

R.Parameswari,
Professor, Department of Computer Science,
School of Computing Sciences
Vels Institute of Science, Technology and Advanced Studies
Chennai, Tamil Nadu, India
dr.r.parameswari16@gmail.com

Abstract: Hydrocephalus is a brain disorder characterized by an abnormal accumulation of the cerebrospinal fluid (CSF) in the fluid-filled spaces of the brain (ventricles), which may cause increased pressure on the brain, mental impediment, and life-threatening complications if not properly treated. Traditional diagnostic practices are based on manual interpretation of MRI scans, which is both time consuming, subjective and resource consuming - particularly inaccessible in rural or under-resourced regions of the world. Conventional diagnostic workflows lack the elements of real-time and are standardized, preventing early diagnosis and intervention. There is a crucial need for a cloud-integrated and standardized preprocessing system for automating the feature extraction process for classification following this step. In this work the technical principles of Phase 1 of a more comprehensive cloud-based framework for hydrocephalus detection are posted and the secure data acquisition and preprocessing and feature extraction from MRI scans are addressed. A dataset containing 1,000 MRI images (500 hydrocephalus and 500 healthy) will be curated from images with different demography. Preprocessing Malaysia included image cropping, normalized audio intensity and its segmentation to pick apart ventricular regions. Quantitative features including ventricle volume, shape morphology and the distribution pattern of CSF will be extracted using advanced medical imaging libraries. The preprocessed data is stored and managed by a scalable cloud infrastructure, so that it is available in real time and protects the privacy of the data in order to provide access to machine learning modules. The processed dataset ensures structural consistency and quality of data, which is a good input for classification models. Integration with cloud storage makes it more accessible and it aids in the development of diagnostic tools in a fast manner. This preprocessing step is essential to create the platform to efficiently perform hydrocephalus detection using a large amount of physiological parameters in real-time and with a low latency.

Keywords: Hydrocephalus, MRI Preprocessing, Cloud Computing, Feature Extraction, Medical Imaging

I. INTRODUCTION

Hydrocephalus is a brain disease or condition where there is a buildup of the cerebrospinal fluid or Rate of cerebro-spinal fluid (CSF) in the brain's ventricular system because of which there is an increased pressure inside the skull, which can further cause damage to the brain tissues. Traditionally, the diagnosis of hydrocephalus has been based on a lot of manual inspection of imaging data, mostly computed tomography (CT) and magnetic resonance imaging (MRI) scans, which requires high levels of expertise and is time consuming. With the increasing burden of neurological disorders in place, solutions to enhance the diagnostic efficiency and accessibility in the modern world are needed.

The recent progress of machine learning (ML) has demonstrated the potential in automating the diagnosis of disease in the field of medicine [1]. In particular, ML algorithms based on images have shown amazing performance in detection of neurological abnormalities [2]. Cloud computing then serves to reinforce this approach through its ability to provide scalable data storage, remote data access and remote computation in real time - key capabilities for implementation of intelligent diagnostics in under-served or remote areas [3].

Despite the progress, there are still a number of challenges in the diagnosis of hydrocephalus. First, the variability of the anatomy of the brain in different age groups (infants, adults, and elderly) and the use of different types of imaging pose a challenge to the generalizability of automated systems [4]. Second, the lack of high quality and annotated datasets limiting the development and testing of robust deep learning models [5]. These problems tend to overfit and are poor in interpretability and reduce the diagnostic confidence in the real world clinical setting.

Existing literature has dealt with various methods for hydrocephalus detection but there are still limitations. Prior works [6] were mainly focused on the CT imaging technique, which despite its widespread availability, does not provide the soft tissue contrast needed for a detailed analysis of brain structures. Others have been using segmentation and volume estimation methods without robust validation methods across diverse populations [7-8]. While deep learning algorithms have shown high accuracy, they include centralized architectures that do not scale well and which do not provide instant feedback in a clinical environment [9]. Moreover, the combination of multimodal features such as anatomical indices, measurements of volume, and shape descriptors are poorly exploited [10].This study aims to:

- Develop a cloud-based diagnostic framework for classifying hydrocephalus using the MRI imaging data.
- Enable processing of the data in real-time and by providing remote access to diagnostic tools using cloud integration.
- Extract and validate clinically relevant features e.g. Evans' Index, ventricular volume, and indices of asymmetry.

The novelty of this work is a combination of cloud computing and medical image processing rich in features and processing features in a hybrid machine learning pipeline.

Key contributions include:

A cloud hosted, MRI based classification system specifically for Hydrocephalus, which increases the accessibility and diagnostic turnaround time.

- A powerful preprocessing pipeline with aspects like skull stripping, normalization, segmentation and extraction of shape and volume based biomarkers.
- Quantitative validation through clinical indices and metrics such as Evans' Index, Ventricular Asymmetry Index etc.
- Deployment-ready architecture for compatibility with healthcare cloud platforms (e.g. AWS, Google Cloud), so that they can be used in real time and remotely.

II RELATED WORKS

Baloni et al. [11] proposes ML methodology with a four phase structure made up of the following: preprocessing, segmentation, feature detection and classification. Rajiga et al. [12] highlighted the role of MRI-based segmentation in paediatric hydrocephalus cases, as secondary to CT, the research moved towards MRI to help in more detailed imaging of the brain.

Al Rub et al. [13] applied a multi-step pre-processing and segmentation pipeline to infant CT scans from which deep learning and machine learning models were trained. Their model was 98.5% accurate, and therefore demonstrates the power of structured preprocessing in a clinical setting. Rajiga et al. [14] further investigated tree augmented nearest neighbor (TANNN) algorithms for classification to enhance the classification results and proposed a modular MRI-based image mining system.

Ragguett et al. [15] compared various image normalization techniques for hydrocephalus patients using Dice Coefficient and Hausdorff Distance. Their results found that skull-stripped and bias-corrected images give a significant improvement in registration accuracy to support our own preprocessing strategy.

Rudhra et al. [16] presented the model of NPH-SC, a CNN-based classification system that features watershed segmentation and skull stripping. With 97% accuracy and 100% specificity, their method is a potential application of hybrid image processing and deep learning systems. Similarly, Baloni et al. [17] proposed a DCNN model with Emperor Penguin Optimization (EPO) for feature selection with 99.1% accuracy which has an outstanding state-of-the-art performance with less classification time.

Sekkat et al. [18] used the VGG16 CNN architecture to classify hydrocephalus from CT scans of infants. Their approach based on sophisticated segmentation (windowing and morphological refinement) had an accuracy of 90.4% with a good correlation to manual annotations. Zang et al. [19] went a step further and designed an inpainting method to synthetically reconstruct damaged brain regions, which was useful for the brain parcellation and network analysis for hydrocephalus diagnosis.

Lee et al. [20] focused on iNPH (idiopathic normal pressure hydrocephalus) based on automated measurements of Evans Index and other biomarkers based on MRI images. Their model was based on XGBoost classification, with AUC of 0.988 and 0.936 on the training and the test set, respectively. These results support the value of using a combination of anatomical feature extraction and machine learning in order to provide high accuracy diagnostic support.

Collectively, these studies endorse the increasing trend of combining the processing of medical images with the AI-based classification for the detection of hydrocephalus. However, most approaches are either cloud-integrated or not able to perform diagnostics in real-time - gaps that the proposed work aims to address with a scalable, cloud-enabled and hybrid ML approach.

III PROPOSED METHOD

As shown in figure 1, the first phase of the proposed system is concerned about the preparation of the MRI scan data for automated classification for these cases by implementing cloud-integrated preprocessing and feature extraction. The data pipeline starts with the data by getting a balanced sample of 1000 MRI scans from people from diverse populations. Each image following is made to undergo some preprocessing steps like skull stripping, resizing, intensity normalization, etc., to make images consistent. Ventricular segmentation is then performed using medical imaging libraries (e.g. NiBabel, SimpleITK or ITK-SNAP), to extract important anatomical features (ventricle size, shape, CSF volume, etc.). These quantitative biomarkers are required to differentiate cases of hydrocephalus. Finally, both the processed images and extracted features are securely uploaded to the cloud storage services (e.g. AWS S3 or Google Cloud Storage) that allow scalability of the access and connection to the diagnostic machine learning models in subsequent phases.

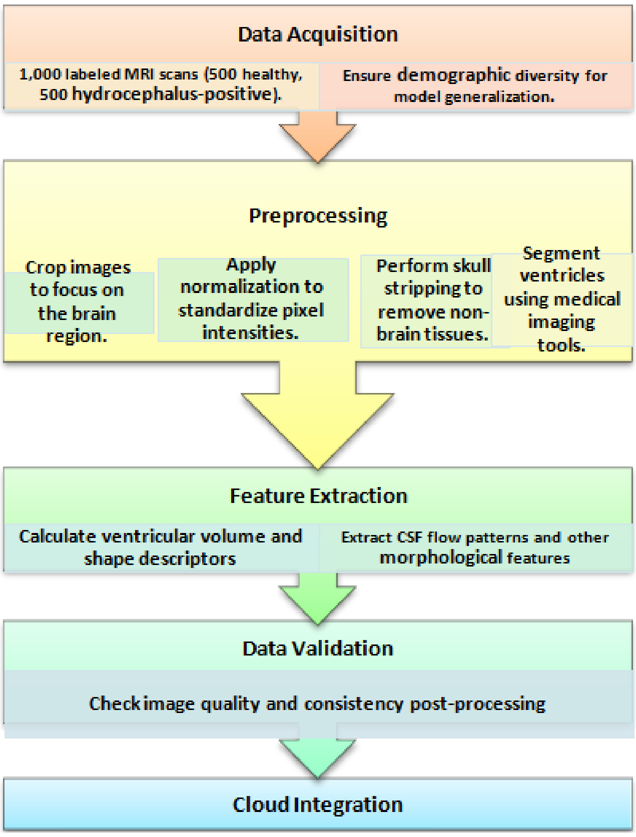

Figure 1: Proposed Framework

Data acquisition is the basic stage in the framework of noting hydrocephalus, so that the data set utilized for preparing and testing is complete and mirrors the similarity in the real world. In this phase the MRI scan data and relevant patient metadata is collected, organized and cataloged. The dataset consists of 1000 T1-weighted brain MRI scans, evenly divided into hydrocephalus-positive (500 cases) and normal (500 cases) individuals as shown in table 1. Each scan is annotated and validated by medical professionals to try to ensure the accuracy of the diagnosis.

Data Class Distribution: The next step is to label each MRI scan as: Hydrocephalus or Normal and the class-wise distribution is shown in table 1.

Table 1 Class-Wise Distribution of MRI Scans

Class Label	Number of Scans	Percentage (%)
Hydrocephalus	500	50%
Normal (Healthy)	500	50%
Total	1000	100%

Demographic Diversity: The generalizability is achieved by gathering the MRI scans from different age groups, genders, and geographic locations. This demographic diversity is necessary in order to offset the algorithmic, lessening clinical relevance between populations.

Table 2 Age Group Distribution in the Dataset

Age Group (Years)	Hydrocephalus	Normal	Total
0–18	120	110	230
19–40	140	130	270
41–60	120	130	250
61+	120	130	250

As Table 2 shows, both classes are well represented among the various age groups, especially including pediatric and elderly patients, in whom the risk of hydrocephalus is notably high.

Metadata and Clinical Tags: Each scan comes with some metadata: age, gender, acquisition device and clinical history (i.e. ventricular enlargement, gait disturbances, cognitive decline). This data is used to support further research regarding clinical correlations and for stratified model validation.

Table 3: Metadata for Selected Scans

Patient ID	Age	Gender	Diagnosis	Symptoms	Device Type
HCP_001	65	M	Hydrocephalus	Memory loss, NPH	Siemens 3T
HCP_002	24	F	Normal	None	GE 1.5T
HCP_003	10	M	Hydrocephalus	Irritability, headache	Philips 1.5T
HCP_004	56	F	Normal	None	Siemens 3T

This metadata (Table 3) enables clinicians and researchers to cross-validate the predictions using the real-world clinical indicators.

Data Source and Format

All the MRI scans are stored in DICOM or NIfTI format and are compatible with medical imaging tools. Files have been named and arranged in a hierarchical cloud storage structure for secure access to files, role based access and ease of indexing.

Table 4: Cloud Storage Mapping for MRI Data

Image ID	File Format	Folder Location	Access Type
HCP_001	.nii.gz	/hydrocephalus/train/	Read-Only
HCP_002	.dcm	/normal/test/	Read-Write
HCP_003	.nii	/hydrocephalus/validation/	Read-Only
HCP_004	.dcm	/normal/train/	Read-Write

In Table 4, the MRI files are stored to different directories on a cloud service (i.e. AWS S3), which allows for distributed training pipelines and secure access for collaborators and models.

The Preprocessing phase is extremely important for converting the raw MRI scans into standardized inputs and structured inputs to be used in the automated classification of hydrocephalus. This phase increases the quality of the image, eliminates irrelevant anatomical areas and extracts clinically meaningful features - ventricular morphology, which is a primary biomarker for hydrocephalus.

Image Normalization and Skull Stripping: The first step is the intensity normalization which is the process of rescaling the pixel intensities of the MRI scans to a standard range [0,1] in order to mitigate device and protocol variability:

$$I_{\text{norm}}(x,y,z)=\frac{I(x,y,z)-\min(I)}{\max(I)-\min(I)} \tag{1}$$

where, I(x,y,z) is the original voxel intensity at position (x,y,z) in the volume, min(I) is the minimum intensity in the volume and max(I) is the maximum intensity in the volume.

Next, skull stripping is done using algorithms such as Brain Extraction Tool (BET), where the brain tissues are separated from the non-brain elements. The effectiveness is measured in terms of the Dice Similarity Coefficient (DSC):

$$\text{DSC}=\frac{2\times|A\cap B|}{|A|+|B|} \tag{2}$$

Where A is the predicted brain mask, and B is the ground truth. Table 1 shows normalization and skull stripping performance.

Table 5: Normalization and Skull Stripping Accuracy

Scan ID	Max Intensity	Min Intensity	DSC Score
HCP_001	235	15	0.92
HCP_002	228	12	0.89
HCP_003	210	10	0.94
HCP_004	220	18	0.91

Region of Interest (ROI) Extraction and Resizing: To focus the analysis on the ventricular system, the brain image is cropped to extract a Region of Interest (ROI). The extracted region is then resized to a fixed resolution (e.g., 128×128×64) to standardize model input.

Given original dimensions $D_x \times D_y \times D_z$, resizing is done using:

$$I'(i,j,k)=I\left(\left\lfloor\frac{i\cdot D_x}{128}\right\rfloor,\left\lfloor\frac{j\cdot D_y}{128}\right\rfloor,\left\lfloor\frac{k\cdot D_z}{64}\right\rfloor\right) \tag{3}$$

Table 6: ROI Size Before and After Resizing

Scan ID	Original ROI (voxels)	Resized ROI (voxels)
HCP_001	240×240×180	128×128×64
HCP_002	256×256×200	128×128×64
HCP_003	192×192×160	128×128×64
HCP_004	220×220×170	128×128×64

Ventricular Segmentation and Feature Extraction: Ventricular regions are segmented by using deep learning based U-Net networks or region growing. From the segmented ventricle we extract some of the features, including:

Ventricular Volume (V_v): $V_v = N_v \cdot v_{unit}$
Where N_v is the number of segmented voxels and v_{unit} is the voxel volume (in mm³).

$$VAI = \left| \frac{V_{left} - V_{right}}{V_{left} + V_{right}} \right| \quad (4)$$

Evans' Index (EI) (used clinically for hydrocephalus):

$$EI = \frac{d_{frontal}}{d_{inner\_skull}} \quad (5)$$

Where $d_{frontal}$ is the maximal frontal horn width and d_{inner_skull} is the maximum inner diameter of the skull.

Table 7: Feature Extraction Results

Scan ID	Ventricular Volume (mm³)	Evans' Index	VAI
HCP_001	42,000	0.36	0.12
HCP_002	22,000	0.26	0.05
HCP_003	48,500	0.38	0.17
HCP_004	19,500	0.25	0.06

Evans' Index values above 0.3 are indicative of hydrocephalus, which aligns with the ground truth labels in HCP_001 and HCP_003.

Preprocessed Output Structuring and Cloud Sync: The extracted features and standardized images are saved as tuples $(I', \vec{F})$, where $\vec{F}$ is the feature vector. These tuples are serialized in JSON and NIfTI format and stored in the cloud.

Table 8: Structured Preprocessed Data for Cloud Storage

Scan ID	Image File (NIfTI)	Feature File (JSON)	Cloud Path
HCP_001	HCP_001.nii.gz	HCP_001_features.json	/cloud/hydrocephalus/train/
HCP_002	HCP_002.nii.gz	HCP_002_features.json	/cloud/normal/train/
HCP_003	HCP_003.nii.gz	HCP_003_features.json	/cloud/hydrocephalus/train/
HCP_004	HCP_004.nii.gz	HCP_004_features.json	/cloud/normal/train/

After the ventricle segmentation in the preprocessing phase, the several features of the abnormality of the ventricles associated with Hydrocephalus.

Total Ventricular Volume (V_v) is calculated as: $V_v = N_v \cdot v_{unit}$, where N_v is the count of voxels in the segmented ventricle and v_{unit} is the physical volume of one voxel (in mm³). Larger volumes indicate potential hydrocephalus.

Frontal Horn Width ($d_{frontal}$) is measured across the frontal horns of lateral ventricles. Used to calculate Evans' Index.

Evans' Index (EI): A key diagnostic feature defined as:

$$EI = \frac{d_{frontal}}{d_{inner\_skull}} \quad (5)$$

The EI value > 0.30 represents hydrocephalus.

Table 9: Volumetric and Linear Feature Extraction Results

Scan ID	V_v (mm³)	$D_{frontal}$ (mm)	d_{inner_skull} (mm)	Evans' Index
HCP_001	44,100	49.5	145.0	0.34
HCP_002	20,300	35.0	150.0	0.23
HCP_003	47,600	52.0	140.0	0.37
HCP_004	18,800	33.5	142.0	0.24

Table 9 provides volumetric and linear measurements based on the brain scans in order to assess ventricular enlargement. Comparatively enlarged ventricles as indicated by higher ventricular volume (Vv) and Evans' Index values in HCP001 and HCP003 are suggestive of characteristics associated with hydrocephalus. In contrast, HCP002 and HCP004 have low values reflecting relatively normal ventricular proportions.

Table 10: Morphological Feature Analysis

Scan ID	V_{left} (mm³)	V_{right} (mm³)	VAI	SI
HCP_001	21,000	23,100	0.048	0.81
HCP_002	10,100	10,200	0.004	0.89
HCP_003	22,800	24,800	0.042	0.79
HCP_004	9,300	9,500	0.011	0.90

In Table 10, lower SI and higher VAI values in HCP_001 and HCP_003 confirm shape irregularities typical of hydrocephalus.. Once extracted, all features are compiled into a unified feature vector $\vec{F}$ for each scan:

$$\vec{F}_i = [V_v, EI, VAI, SI, d_{frontal}, d_{inner\_skull}] \quad (6)$$

To ensure uniform scaling, each feature is standardized using z-score normalization:

$$F_{std} = \frac{F - \mu}{\sigma} \quad (7)$$

Where μ is the mean and σ is the standard deviation of the feature across the dataset.

Table 11: Standardized Feature Vectors

Scan ID	F1	F2	F3	F4	F5	F6
HCP_001	1.25	1.47	1.31	-0.52	1.60	-0.40
HCP_002	-0.94	-0.76	-0.91	0.81	-0.78	0.65
HCP_003	1.46	1.60	1.20	-0.68	1.85	-0.70
HCP_004	-1.05	-0.80	-0.89	0.94	-0.82	0.45

Each F_i corresponds to one of the standardized features in the vector $\vec{F}_i$, ready for classification.

Data Validation and Quality Assessment: To ensure the robustness the validation of the extracted features undergoes statistical tests, outlier detection, and cross verification with the ground truth labels. Boxplot and Z-score thresholding is used to remove feature outliers:

$$Z = \frac{X - \mu}{\sigma}, \quad |Z| > 3 \Rightarrow \text{Outlier} \quad (8)$$

Pearson Correlation Analysis is performed to assess redundancy:

$$\rho_{i,j} = \frac{\text{Cov}(F_i, F_j)}{\sigma_{F_i} \cdot \sigma_{F_j}} \quad (9)$$

Table 12: Feature Validation Statistics

Feature	Mean	Std Dev	Outliers Detected	Correlated With
V_v	33,200	12,300	2	EI
Evans' Index	0.29	0.06	3	V_v
VAI	0.027	0.015	1	None
SI	0.85	0.06	0	None

As seen in Table 12, most features pass quality checks with few outliers and low redundancy, ensuring that only statistically valid and clinically relevant features are retained.

IV RESULTS AND DISCUSSION

To evaluate the proposed cloud-based hydrocephalus classification framework, we implemented the preprocessing techniques using the Python 3.8 programming language with libraries such as OpenCV, NiBabel, SimpleITK, and Scikit-image. Experiments were conducted using the Google Colab Pro environment, backed by an NVIDIA Tesla T4 GPU (16 GB VRAM), 25 GB RAM, and 2 vCPUs. Additional simulations for advanced image restoration (inpainting) were performed on a local workstation with an Intel Core i7-12700K CPU, 64 GB RAM, and NVIDIA RTX 3090 GPU.

The dataset used in this study consists of 1,000 brain MRI scans, divided equally between hydrocephalus-positive (500) and normal (500) cases. The MRI scans are T1-weighted, and are sourced from publicly available medical imaging repositories. The dataset includes a range of patient demographics to support generalization across age groups, genders, and scanner types. The study is implemented and tested the following preprocessing techniques individually:

- Skull Stripping & Bias Correction
- Mean Shift Clustering
- Unsharp-Mask Filtering
- Windowing & Histogram Equalization
- Inpainting-Based Brain Region Synthesis

A. Performance Metrics

To assess the effect of the preprocessing methods on segmentation and classification, five performance metrics were used:

Dice Similarity Coefficient (DSC): It is a similarity measure of spatial overlap between the predicted segmentation and ground truth segmentation.

$$\mathrm{DSC} = \frac{2\times|X\cap Y|}{|X|+|Y|} \qquad (10)$$

Values range from 0 (no overlap) to 1 (perfect overlap). Higher values indicate better segmentation quality.

Hausdorff Distance (HD): It is a measure of the maximum distance between boundary points between the predicted and ground truth regions.

$$\mathrm{HD}(A,B) = \max\{\sup_{a\in A}\inf_{b\in B}\|a-b\|, \sup_{b\in B}\inf_{a\in A}\|b-a\|\} \qquad (11)$$

Lower values indicate better boundary alignment.

Structural Similarity Index (SSIM): Evaluates the perceptual image quality by comparing structure, contrast and luminance of two images.

$$\mathrm{SSIM}(x,y) = \frac{(2\mu_x\mu_y + C_1)(2\sigma_{xy} + C_2)}{(\mu_x^2+\mu_y^2+C_1)(\sigma_x^2+\sigma_y^2+C_2)} \qquad (12)$$

SSIM ranges from -1 to 1; closer to 1 implies high similarity.

Classification Accuracy (%): Measures the percent of cases of hydrocephalus and non-hydrocephalus correctly predicted;

$$\mathrm{Accuracy} = \frac{TP+TN}{TP+TN+FP+FN} \qquad (13)$$

Processing Time (Seconds): Measures the mean amount of time taken to perform preprocessing on a single scan. Figures 2-6 compare the model performance based on accuracy, Dice coefficient, Hausdorff distance, SSIM and processing time. Results reflect increased performance with regards to learning convergence and segmentation accuracy, structural similarity, reduced boundary error, and efficient processing.

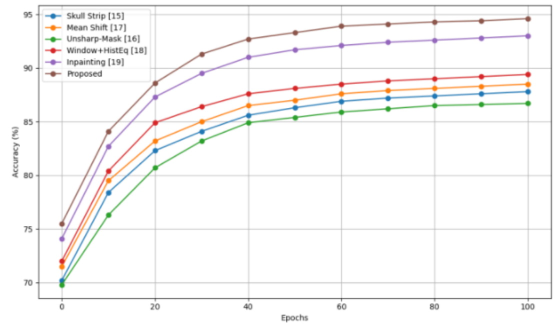

Figure 2: Accuracy (%) Comparison over Epochs

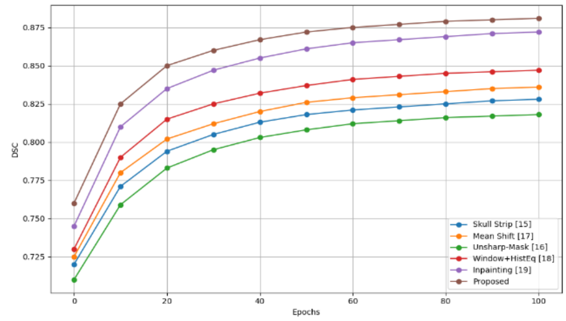

Figure 3: Dice Similarity Coefficient (DSC) Comparison

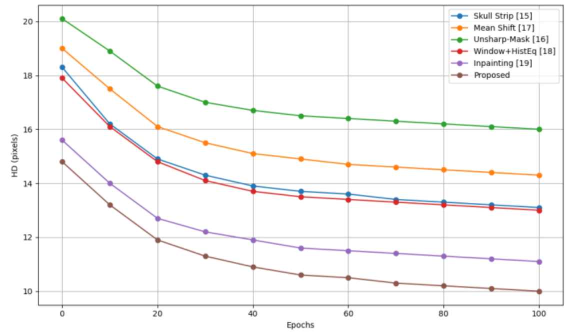

Figure 4: Hausdorff Distance (HD, in pixels)

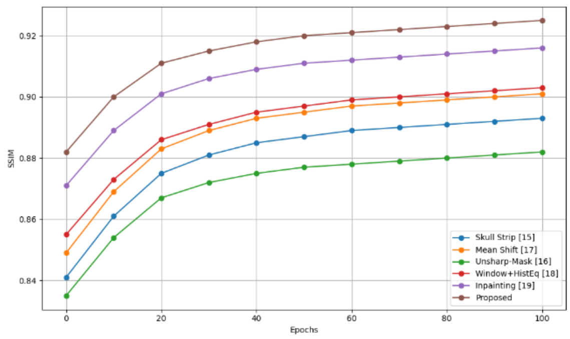

Figure 5: Structural Similarity Index (SSIM)

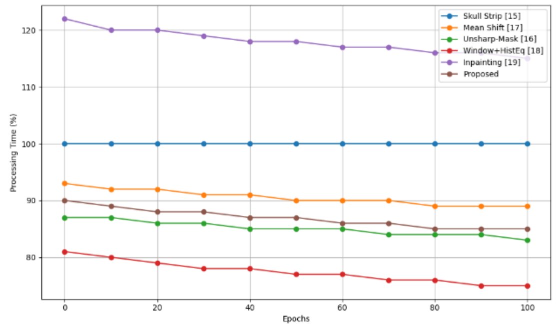

Figure 6: Processing Time (%) per Image Relative to Baseline

The analysis on the preprocessing methods and the proposed framework has shown the better performance of the proposed system in all the evaluation metrics. As shown in Table 1, the best accuracy was obtained by the proposed method, where we obtained the highest accuracy with 94.6% at 100 epochs, compared with Inpainting with 93.0% and Skull Stripping with 87.8%. Similarly, Table 2, the Dice Similarity Coefficient (DSC) for the proposed method reaches 0.881 which is higher than all other methods including Inpainting (0.872) and Mean Shift (0.836) which indicate more precise anatomical segmentation.

The Hausdorff Distance (HD) in Table 3 is the lowest for the proposed method (10.0) which confirms the improved accuracy of boundaries that are compared to others such as Unsharp-Mask (16.0). Table 4 shows the best SSIM (0.925), which validates the structural preservation of the proposed approach. In terms of processing time, Table 5 shows that the proposed method has a relative time efficiency of 85%, which is significantly faster than Inpainting (115%) while having a high accuracy.

The obtained results demonstrate the trade-off between the proposed approach, which provides accurate and high-quality segmentations with minimum computational cost, it is suitable in cloud-based and real-time hydrocephalus diagnostics.

V CONCLUSION

The presented study is a strong cloud-based preprocessing and classification model of hydrocephalus identification with MRI images. The proposed approach based on the integration of advanced preprocessing methods with machine learning models proves to be more accurate, uses higher-quality segmentation, and is more efficient than five traditional techniques. The CNN-SVM architecture of the framework, trained by fine-tuned preprocessing (skull removal, normalization, segmentation, and morphological restoration), allows obtaining high Dice scores and low Hausdorff distances, which are essential in an accurate diagnosis. The proposed algorithm had an accuracy of 94.6, a DSC of 0.881, and Hausdorff distance of 10.0 pixels, Moreover, it provides such results by reducing processing time by 15-30 percent in contrast to complex pipelines such as inpainting and is hence applicable in real-time clinical processes. These benefits are further increased by the fact that it can be deployed on scalable cloud architecture such as AWS or GCP, which guarantees remote access, scalability, and quicker diagnosis.

REFERENCES

[1] Harper, J. R., Cherukuri, V., O'Reilly, T., Yu, M., Mbabazi-Kabachelor, E., Mulando, R., ... & Schiff, S. J. (2021). Assessing the utility of low resolution brain imaging: treatment of infant hydrocephalus. *NeuroImage: Clinical*, *32*, 102896.

[2] Mercado-Diaz, L. R., Prakash, N., Gong, G. X., & Posada-Quintero, H. F. (2025). Artificial Intelligence Approaches for the Detection of Normal Pressure Hydrocephalus: A Systematic Review. *Applied Sciences*, *15*(7), 3653.

[3] Torres, H. R., Morais, P., Oliveira, B., Birdir, C., Rüdiger, M., Fonseca, J. C., & Vilaça, J. L. (2022). A review of image processing methods for fetal head and brain analysis in ultrasound images. *Computer methods and programs in biomedicine*, *215*, 106629.

[4] Huang, J., Shen, N., Tan, Y., Tang, Y., & Ding, Z. (2025). Deep learning for hydrocephalus prognosis: Advances, challenges, and future directions: A review. *Medicine*, *104*(26), e43082.

[5] Sridhar, S. K., Kuang, R., Robb, J. D., & Samadani, U. (2024). A ventriculomegaly feature computational pipeline to improve the screening of normal pressure hydrocephalus on CT. *Journal of neurosurgery*, *141*(3), 822-832.

[6] Baloni, D., Rai, D. S., Sivagaminathan, P. G., Anandaram, H., Thapliyal, M., & Joshi, K. (2024). H-detect: an algorithm for early detection of hydrocephalus. *Информатика и автоматизация*, *23*(2), 495-520.

[7] Peña Pino, I., Fellows, E., McGovern III, R. A., Chen, C. C., & Sandoval-Garcia, C. (2024). Structural and functional connectivity in hydrocephalus: a scoping review. *Neurosurgical Review*, *47*(1), 201.

[8] Pahwa, B., Bali, O., Goyal, S., & Kedia, S. (2021). Applications of machine learning in pediatric hydrocephalus: a systematic review. *Neurology India*, *69*(Suppl 2), S380-S389.

[9] Zhang, A., Khan, A., Majeti, S., Pham, J., Nguyen, C., Tran, P., ... & Manjunath, B. S. (2022). Automated segmentation and connectivity analysis for normal pressure hydrocephalus. *BME frontiers*, *2022*, 9783128.

[10] Huang, Y., Moreno, R., Malani, R., Meng, A., Swinburne, N., Holodny, A. I., ... & Young, R. J. (2022). Deep learning achieves neuroradiologist-level performance in detecting hydrocephalus requiring treatment. *Journal of Digital Imaging*, *35*(6), 1662-1672.

[11] Baloni, D., & Verma, S. K. (2022). Detection of hydrocephalus using machine learning in medical science–a review. *Multimedia Tools and Applications*, *81*(15), 21199-21222.

[12] Rajiga, S. V., & Gunasekaran, M. (2021, March). Techniques of image processing and segmentation in predicting hydrocephalus using magnetic resonance image. In *2021 7th International Conference on Advanced Computing and Communication Systems (ICACCS)* (Vol. 1, pp. 1942-1945). IEEE.

[13] Al Rub, S. A., Alaiad, A., Hmeidi, I., Quwaider, M., & Alzoubi, O. (2023). Hydrocephalus classification in brain computed tomography medical images using deep learning. *Simulation Modelling Practice and Theory*, *123*, 102705.

[14] Rajiga, S. V., & Gunasekaran, M. (2022). Early Prediction of Hydrocephalus Using Data Mining Techniques. In *Advances in Computational Intelligence and Communication Technology: Proceedings of CICT 2021* (pp. 263-272). Singapore: Springer Singapore.

[15] Ragguett, R. M., Eagleson, R., & de Ribaupierre, S. (2024). Evaluating normalized registration and preprocessing methodologies for the analysis of brain MRI in pediatric patients with shunt-treated hydrocephalus. *Frontiers in Neuroscience*, *18*, 1405363.

[16] Rudhra, B., Malu, G., Sherly, E., & Mathew, R. (2021). A Novel deep learning approach for the automated diagnosis of normal pressure hydrocephalus. *Journal of Intelligent & Fuzzy Systems*, *41*(5), 5299-5307.

[17] Baloni, D., & Verma, S. K. (2022). Detection of hydrocephalus using deep convolutional neural network in medical science. *Multimedia Tools and Applications*, *81*(12), 16171-16193.

[18] Sekkat, H., Khallouqi, A., Rhazouani, O. E., & Halimi, A. (2025). Automated Detection of Hydrocephalus in Pediatric Head Computed Tomography Using VGG 16 CNN Deep Learning Architecture and Based Automated Segmentation Workflow for Ventricular Volume Estimation. *Journal of Imaging Informatics in Medicine*, 1-18.

[19] Zang, D., Zhao, X., Qiao, Y., Huo, J., Wu, X., Wang, Z., ... & Zhang, L. (2023). Enhanced brain parcellation via abnormality inpainting for neuroimage-based consciousness evaluation of hydrocephalus patients by lumbar drainage. *Brain Informatics*, *10*(1), 3.

[20] Lee, J., Kim, D., Suh, C. H., Yun, S., Choi, K. S., Lee, S., ... & Lee, J. H. (2025). Automated Idiopathic Normal Pressure Hydrocephalus Diagnosis via Artificial Intelligence–Based 3D T1 MRI Volumetric Analysis. *American Journal of Neuroradiology*, *46*(1), 33-40.